Materials Science Forum Vols. 338-342 (2000) pp. 477-480
© 2000 Trans Tech Publications, Switzerland

Origin of Threading Dislocation Arrays in SiC Boules Grown by PVT

S. Ha, N.T. Nuhfer, M. De Graef, G.S. Rohrer and M. Skowronski

Department of Materials Science and Engineering, Carnegie Mellon University,
5000 Forbes Ave, Pittsburgh, PA 15213, USA

Keywords: Bulk Crystal Growth, Physical Vapor Transport, Polygonization, Slip Bands, Threading Dislocation Array

Abstract

Transmission electron microscopy (TEM), high resolution x-ray diffraction (HRXRD), and KOH etching have been used to study the dislocation structure of 4H SiC crystals grown by physical vapor transport (PVT). Many of the observed etch pits form arrays extending along the $\langle 11\bar{2}0\rangle$ and $\langle \bar{1}100\rangle$ directions on (0001) wafers. Plan view conventional and high resolution TEM show that both types of arrays consist of pure edge dislocations threading along the c-axis with identical Burgers vectors of the $a/3\langle 11\bar{2}0\rangle$ type. The former arrays are interpreted as slip bands formed by dislocation glide in the slip system $\langle 11\bar{2}0\rangle\{\bar{1}100\}$ of hexagonal SiC during post-growth cooling. The latter arrays constitute low angle tilt boundaries with tilt axis parallel to the [0001] direction. Evidence is presented that such boundaries can form by polygonization of the threading edge dislocations introduced by plastic deformation.

Introduction

Two critical issues in the development of substrates for SiC-based electronics are increasing the size of boules and reducing the structural defect density. Of particular interest are extended defects propagating along the [0001] growth direction. Such threading defects are known to penetrate active device layers deposited by epitaxy and to degrade device performance [1, 2].

In previous studies, three characteristic etch pit types were observed on the surfaces of [0001] grown crystals and assigned to three different threading defects, i.e. micropipes, screw dislocations, and threading edge dislocations [3, 4]. In addition, a domain structure was postulated to be related to the distribution of these threading defects [4-6].

Glass *et al.* [5] first postulated the domain structure on the basis of HRXRD data. They showed that ω rocking curves of either symmetric or asymmetric reflections on (0001) SiC wafers exhibit multiple peaks, implying that parts of the crystal are misoriented with respect to others. They suggested that because a SiC crystal grows by the spiral mechanism with numerous independent nuclei, the initial misorientations between nuclei are accommodated in the form of domain walls when the nuclei grow and coalesce. This interpretation was supported by Tuominen *et al.* [6], who showed a well defined domain structure on a KOH etched wafer. Centers of domains exhibit relatively few dislocation etch pits, while the domain walls have high etch pit densities. Further data were provided by Takahashi *et al.* [4]. They concluded, in agreement with the above authors, that domains are grown-in type with most of the defects inherited from the seed or originating at the seed-boule interface. The misorientation between domains was determined to have both twist and tilt components.

In this work, we identified one type of characteristic threading dislocation array and determined its relation with the domain structure. Based on these observations, we propose a new formation mechanism for the dislocations and the domain structure.

Experimental Procedures

The crystals were grown by Cree Research, Inc. (Durham, NC) as a part of the development program on High Temperature Electronics, supported by the Defense Advanced Research Project Agency. Two inch diameter wafers were undoped or n-doped (~10^{18} cm^{-3}) and oriented along (0001) to within 0.5°. KOH etching was applied at 500°C or 510°C for 10 minutes on Si(0001) faces of the wafers. The etch pits were observed using Nomarski-contrast optical microscopy. Laue x-ray diffraction was employed to determine the orientation of etch pit arrays. The TEM observations were carried out on a Philips EM420-TEM and on a JEOL 4000 EX-TEM, operated at 120 and 400 kV, respectively. HRXRD was conducted using Cu $K\alpha_1$ radiation on a Philips MRD diffractometer, equipped with a four bounce monochromator and a two bounce analyzer crystal employing Ge (220) reflection. The angular resolution was better than 0.004° (~14″).

Results and Discussion

Two kinds of linear arrays of small dislocation etch pits were observed. One type was oriented along the $<11\bar{2}0>$ directions and the other was along the $<\bar{1}100>$ directions. The $<11\bar{2}0>$ oriented etch pit arrays usually formed bands approximately 30~200 μm wide, and appeared along the periphery of the boules. An example of such structure is shown in Fig. 1. The wafer edge is visible in the lower right corner and a part of a polytypic inclusion or a misoriented grain is shown in the lower center. Two parallel bands of small etch pits extend vertically. The wider of the two is marked with an arrow. Their extended lengths were about 4 and 10 mm. It is also noticeable that there are several additional poorly defined bands rotated 60° away from the two prominent bands. The etch pit densities of the bands were in the range of $0.5\sim2.2 \times10^6$ cm^{-2}.

The second type, the $<\bar{1}100>$ oriented etch pit arrays form definite single lines (Fig. 2), and spread over the center region almost uniformly up to 3/4 of the radius of a typical two inch wafer. A few large etch pits due to micropipes could also be seen and are marked M. The lines marked S are due to scratches. All three equivalent $<\bar{1}100>$ array directions were observed. The linear etch pit densities along the arrays were on the order of 10^4 cm^{-1}, while the areal etch pit densities away from these arrays were on the order of 10^4 cm^{-2}. The corresponding average distances between neighboring dislocations are on the order of 1 μm and 100 μm, respectively.

Closer inspection of the small etch pits in Fig. 1 and 2 at high magnification revealed that they appear conical in shape with a pointed bottom and circular outline on the wafer surface. Such shape implies that the etch pits are due to threading dislocations extending approximately normal to the (0001) wafer surface. Subsequently, we applied conventional and high resolution TEM to determine the character of the dislocations in both types of arrays [7, 8]. Fig. 3 is a plan view high

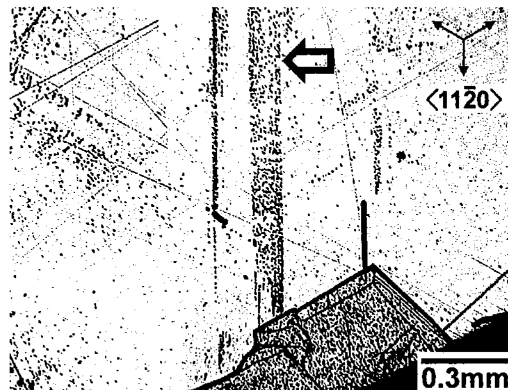

Fig. 1 Optical micrograph of the $<11\bar{2}0>$ etch pit bands on Si(0001) face of a 4H SiC wafer

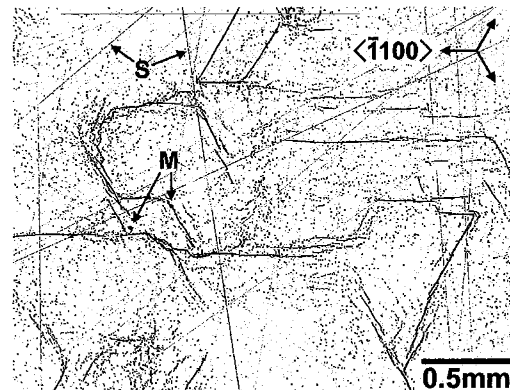

Fig. 2 Optical micrograph of the $<\bar{1}100>$ etch pit arrays on Si(0001) face of a 4H SiC wafer

of the development
ed Research Project
and oriented along
ninutes on Si(0001)
ıl microscopy. Laue
arrays. The TEM
X-TEM, operated at
ı on a Philips MRD
ıce analyzer crystal
·14″).

ıe type was oriented
ıe $\langle 11\bar{2}0\rangle$ oriented
appeared along the
wafer edge is visible
rain is shown in the
wider of the two is
also noticeable that
ʼo prominent bands.

lines (Fig. 2), and
ical two inch wafer.
The lines marked S
ʼed. The linear etch
h pit densities away
ə distances between

n revealed that they
surface. Such shape
ıately normal to the
resolution TEM to
is a plan view high

ıf the $\langle\bar{1}100\rangle$ etch
f a 4H SiC wafer

resolution lattice image around one of the threading dislocations. The image was taken by choosing the c-axis as the zone axis. The dislocation is of the pure edge type and threading along the c-axis without tilt. Its core is at the intersection of the two extra half planes marked with two rows of dots. The corresponding Burgers vector is of the $a/3\langle 11\bar{2}0\rangle$ type with a direction marked by an arrow. The Burgers vectors were identical for all dislocations in an array, and determined to be parallel to the array direction for the $\langle 11\bar{2}0\rangle$ arrays and perpendicular for the $\langle\bar{1}100\rangle$ arrays.

The fact that the pure edge dislocations are aligned in an array parallel to the Burgers vectors suggests that the $\langle 11\bar{2}0\rangle$ arrays were formed by dislocation glide in the corresponding slip system $\langle 11\bar{2}0\rangle\{\bar{1}100\}$. The same slip system in 6H SiC crystals has been observed by Maeda *et al.* [9] to be activated at room temperature by an indentation hardness test. Hence, the slip is expected to occur in the high temperature conditions of PVT growth, at lower stresses than are encountered in the indentation test. As illustrated in Fig. 1, the apparent origin of most slip bands is a misoriented grain or a polytypic inclusion at the periphery of the wafers. Such grains are frequently observed to nucleate on the growth crucible walls. It is plausible to assume that the crystal growing around the misoriented grains is stress free at the growth temperature. During post-growth cooling, the thermal expansion anisotropy between the matrix boule and the misoriented grains leads to stress build-up at the interface as well as inside the grains and the boule. Similarly, any polytypic inclusions would result in stresses due to differences in thermal expansion. As the temperature decreases, the stress will increase until it exceeds the critical resolved shear stress and causes the dislocation glide in the corresponding slip system.

The $\langle\bar{1}100\rangle$ arrays of dislocations which have identical Burgers vectors perpendicular to the array direction can be viewed as low angle grain boundaries. The average distances between neighboring dislocations estimated by TEM were 0.3~1 μm. These correspond to misorientation values of 60~200 arcsec across the arrays, assuming all the dislocations are of same type. The expected type of misorientation is pure tilt with a rotation axis parallel to the c-axis contained in the boundary plane. The type and magnitude of misorientation have been verified by HRXRD experiments [8]. The rotation component around the c-axis across an array was about 140 arcsec, while the other two components corresponding to the misorientation of the basal plane were below 10 arcsec. The arrays frequently formed hexagonal or triangular patterns on the wafer surface as shown in Fig. 2, which is reminiscent of the domain wall pattern reported by Tuominen *et al.* [6]. In this case, the domain walls are made of pure edge threading dislocations with Burgers vectors of the $a/3\langle 11\bar{2}0\rangle$ type. It is worth noting that this kind of domain structure cannot result in misorientations that can be detected in (000n) rocking curves. On the other hand, many authors

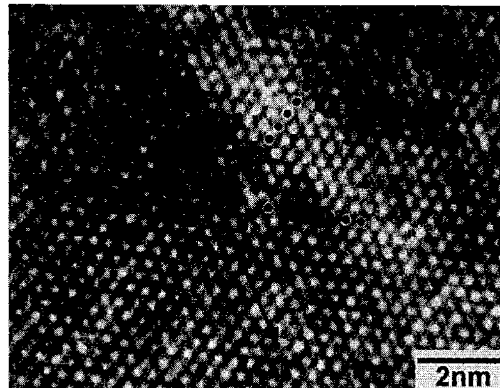

Fig. 3 C-axis plan view lattice image around a threading dislocation in the array of Fig. 1

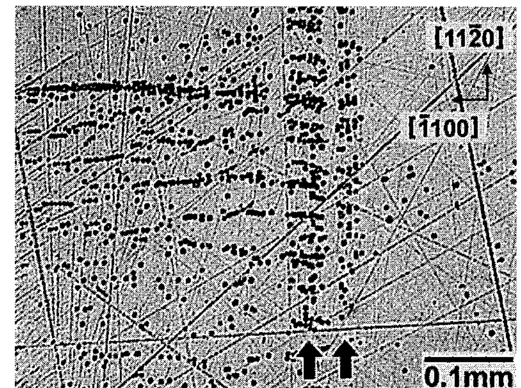

Fig. 4 Optical micrograph of the detail of two slip bands showing partial polygonization

reported multiple peaks present in such reflections. This implies that, in addition to the domain structure described above, there is a different type of boundary with different structure and probably different origin.

The remaining question is the formation mechanism of the domain structure. Presented above is evidence of the activation of the secondary slip system in the PVT growth of SiC crystals. In some cases, slip bands almost reached the center of crystals. Hence, these are major sources of the threading dislocations. In Fig. 4, two slip bands marked with arrows extend vertically. It is clear that etch pits in the bands form fine structure consisting of many small fragments aligned in the direction perpendicular to that of the bands. Since the Burgers vectors of the dislocations within a slip band are identical and parallel to the slip direction, they must be perpendicular to the fragment direction. It is plausible to suggest that the fine structure formation occurred in order to lower the energy of the system. It is well known that the low energy configuration for an array of edge dislocations corresponds to that in which Burgers vectors are perpendicular to the array direction. The alignment process is referred to as polygonization. Fig. 4 shows an initial stage of polygonization of the threading edge dislocations in the slip bands. It is surmised to occur either during post-growth cooling or during post-growth high temperature annealing. It is easy to visualize that if this wafer was subsequently used as a seed in the PVT growth process, the high growth temperature and long time would allow the polygonization to complete. Through glide and/or climb, dislocations introduced by slip could align themselves into the pattern shown in Fig. 2. Thus, we propose that the domain structure of tilt boundaries could be the consequence of plastic deformation of the already solidified crystal followed by dislocation polygonization.

Summary

Threading dislocations forming etch pit arrays along the $\langle\bar{1}100\rangle$ and $\langle 11\bar{2}0\rangle$ directions on Si(0001) faces of [0001] grown crystals were studied. Conventional and high resolution TEM have identified pure edge dislocations lying along the c-axis with Burgers vectors of the $a/3\langle 11\bar{2}0\rangle$ type. Based on relation between the Burgers vectors and the array direction, the $\langle 11\bar{2}0\rangle$ arrays are interpreted as resulting from dislocation glide in the slip system $\langle 11\bar{2}0\rangle\{\bar{1}100\}$ during post-growth cooling. The $\langle\bar{1}100\rangle$ arrays were interpreted as being formed by polygonization of the threading edge dislocations introduced by the slip.

Acknowledgements

This work was supported in part by the Commonwealth of Pennsylvania through the Ben Franklin Technology Center (Grant No. 98W.CM00562R-1) and by National Science Foundation (Grant No. DMR.9903702).

References

[1] P. G. Neudeck, J. A. Powell, IEEE Electron Device Letters **15** (1994), p. 63
[2] P. G. Neudeck, W. Huang, M. Dudley, IEEE Trans. Electron Devices **46** (1999), p. 478
[3] J. Takahashi, M. Kanaya, Y. Fujiwara, J. Crystal Growth **135** (1994), p. 61
[4] J. Takahashi, N. Ohtani, M. Kanaya, J. Crystal Growth **167** (1996), p. 596
[5] R. C. Glass, L. O. Kjellberg, V. F. Tsvetkov, J. E. Sundgren, E. Janzen, J. Crystal Growth **132** (1993), p. 504
[6] M. Tuominen, R. Yakimova, R. C. Glass, T. Tuomi, E. Janzen, J. Crystal Growth **144** (1994), p. 267
[7] S. Ha, N. T. Nuhfer, G. S. Rohrer, M. De Graef, M. Skowronski, submitted to Journal of Electronic Materials (1999)
[8] S. Ha, N. T. Nuhfer, G. S. Rohrer, M. De Graef, M. Skowronski, submitted to Journal of Crystal Growth (1999)
[9] K. Maeda, K. Suzuki, S. Fujita, M. Ichihara, S. Hyodo, Phil. Mag. A **57** (1988), p. 573